# New Iron(II) and Manganese(II) Complexes of Two Ultra-Rigid, Cross-Bridged Tetraazamacrocycles for Catalysis and Biomimicry

**Timothy J. Hubin,[†] James M. McCormick,[†] Simon R. Collinson,[†] Maria Buchalova,[†] Christopher M. Perkins,[§] Nathaniel W. Alcock,[‡] Pawan K. Kahol,[⊥] Ahasuya Raghunathan,[⊥] and Daryle H. Busch*,[†]**

*Contribution from the Department of Chemistry, University of Kansas, Lawrence, Kansas 66045, Department of Chemistry, University of Warwick, Coventry CV4 7AL, England, The Procter & Gamble Company, Cincinatti, Ohio 45202, and Department of Chemistry, Wichita State University, Wichita, Kansas 67208*

*Received February 5, 1999*

**Abstract:** The high-spin dichloro $Mn^{2+}$ and $Fe^{2+}$ complexes of 4,11-dimethyl-1,4,8,11-tetraazabicyclo[6.6.2]-hexadecane (**1**) and 4,10-dimethyl-1,4,7,10-tetraazabicyclo[5.5.2]tetradecane (**2**) provide durable new compounds of these elements for important fundamental studies and applications. The compounds are especially noteable for their exceptional kinetic stabilities and redox activity. The X-ray crystal structures of all four complexes demonstrate that the ligands enforce a distorted octahedral geometry on the metals with two cis sites occupied by labile chloride ligands. Magnetic measurements reveal that all are high spin with typical magnetic moments. Cyclic voltammetry of the complexes shows reversible redox processes at +0.110 and +0.038 V (versus SHE) for the $Fe^{3+}/Fe^{2+}$ couples of Fe(**1**)$Cl_2$ and Fe(**2**)$Cl_2$, respectively, while the $Mn^{3+}/Mn^{2+}$ and $Mn^{4+}/Mn^{3+}$ couples were observed at +0.585 and +1.343 V, and +0.466 and +1.232 V for the complexes Mn(**1**)$Cl_2$ and Mn(**2**)$Cl_2$, respectively. $Mn^{2+}$(**1**) was found to react with $H_2O_2$ and other oxidizing agents to produce the $Mn^{4+}$(**1**) complex. The catalytic efficacy of $Mn^{4+}$(**1**) in aqueous solution has been assessed in the epoxidation reaction of carbamazepine and hydrogen abstraction reaction with 1,4-cyclohexadiene. The complex has been found to be a selective catalyst, exhibiting moderate catalytic activity in oxygen transfer, but significantly more effective catalytic activity in hydrogen abstraction reactions.

## Introduction

Manganese and iron share with copper dominance over the vast realm of redox catalysis in nature, biomimicry, and homogeneous catalysis. Cytochrome P450,[1] catechol dioxygenase,[2] methane monooxygenase,[3] and lipoxygenase[4] display the power and selectivity found in natural iron-based oxidation catalysis while Mn catalase,[5] mitochondrial superoxide dismutase,[6] and Photosystem II[7] similarly illustrate the potency of manganese derivatives. In biomimicry and homogeneous catalysis, porphyrin derivatives have been prominent in the extensive development of catalytically effective iron and manganese derivatives. The quest for functional models for the challenging functions of bleomycin[8] and methane monoxygenase, Photosystem II, and others has fueled the exploration of broad varieties of ligands, with early work focusing on Schiff base ligands of the salen family[9] followed by more diverse ligands, including many studies on dinuclear derivatives in analogy to methane monooxygenase, Mn catalase, and ribonucleotide reductase.[10] From these and other beginnings, important catalysts have emerged, and again many of them are porphyrin derivatives, the most successful being those bearing bulky substituents at the $\alpha$, $\beta$, $\gamma$, and $\delta$ positions or having extensive halogen substituents.[11] In terms of applications, certain derivatives of manganese salen stand out from among the *nonporphyrin* derivatives.[9,12]

[†] University of Kansas.
[‡] University of Warwick.
[$] The Procter & Gamble Company.
[⊥] Wichita State University.

(1) Ortiz de Montellano, P. R., Ed. *Cytochrome P450: Structure, Mechanism, and Biochemistry*; Plenum Press: New York, 1986.
(2) (a) Jang, H. G.; Cox, D. D.; Que, L., Jr. *J. Am. Chem. Soc.* **1991**, *113*, 9200. (b) Han, S.; Eltis, L. D.; Timmis, K. N.; Muchmore, S. W.; Bolin, J. T. *Science* **1995**, *270*, 976.
(3) (a) Waller, B. J.; Lipscomb, J. D. *Chem. Rev.* **1996**, *96*, 2625. (b) Rosenzweig, A. C.; Nordlund, P.; Takahara, P. M.; Frederich, C. A.; Lippard, S. J. *Chem. Biol.* **1995**, *2*, 409. (c) Que, L., Jr.; Dong, Y. *Acc. Chem. Res.* **1996**, *29*, 190.
(4) Boyington, J. C.; Gaffney, B. J.; Amzel, L. M. *Science* **1993**, *260*, 1482.
(5) (a) Pecoraro, V. L., Ed. *Manganese Redox Enzymes*; VCH: New York, 1992. (b) Vainshtein, B. K.; Melik-Adayamyan, W. R.; Barynin, V. V.; Vagin, A. A.; Grebenko, A. I. *Proc. Int. Symp. Biomol. Struct. Interact., Suppl. J. Biosci.* **1985**, *8*, 471. (c) Barynin, V. V.; Vagin, A. A.; Melik-Adayamyan, W. R.; Grebenko, A. I.; Khangulov, S. V.; Popov, A. N.; Andrianova, M. E.; Vainshtein, B. K. *Dokl. Akad. Nauk, SSSR* **1986**, *228*, 877. (d) Weighardt, K.; *Angew. Chem., Int. Ed. Engl.* **1989**, *28*, 1153.
(6) (a) Ludwig, M. L.; Metzger, A. L.; Pattridge, K. A.; Stallings, W. C. *J. Mol. Biol.* **1991**, *219*, 335. (b) Borgstahl, G. E. O.; Parge, H. E.; Hickey, M. J.; Beyer, W. F., Jr.; Hallewell, R. A.; Tainer, J. A. *Cell* **1992**, *71*, 107.
(7) (a) Prosperpio, D. M.; Hoffman, R.; Dismukes, G. C. *J. Am. Chem. Soc.* **1992**, *114*, 4374. (b) Ono, T.; Noguchi, T.; Inoue, Y.; Kusunoki, M.; Matsushita, T.; Oyanagi, H. *Science* **1992**, *258*, 1335. (c) Bossek, U.; Weyhermüller, T.; Weighardt, K.; Nuber, B.; Weiss, J. *J. Am. Chem. Soc.* **1990**, *112*, 6387.
(8) Stubbe, J.; Kozarich, J. W. *Chem. Rev.* **1987**, *87*, 1107.
(9) (a) Srinirason, K.; Perier, S.; Kochi, J. *J. Am. Chem. Soc.* **1986**, *108*, 2309. (b) Zhang, W.; Loebach, J. L.; Wilson, S. R.; Jacobsen, E. N. *J. Am. Chem. Soc.* **1990**, *112*, 2801. (c) Ire, R.; Ito, Y.; Katsuk, T. *Synlett* **1991**, 265. (d) Robert, A.; Tsapara, A.; Meunier, B. *J. Mol. Catal.* **1993**, *85*, 13.
(10) Nordlund, P.; Eklund, H. *J. Mol. Biol.* **1993**, *232*, 123.
(11) (a) Groves, J. T.; Nemo, T. E. *J. Am. Chem. Soc.* **1983**, *105*, 5786. (b) Collman, J. P.; Zhang, X.; Lee, V. J.; Uffelman, E. S.; Brauman, J. I. *Science* **1993**, *261*, 1404.
(12) Jacobsen, E. N.; Zhang, W.; Muci, A. R.; Ecker, J. R.; Deng, L. *J. Am. Chem. Soc.* **1991**, *113*, 7063.

10.1021/ja990366f CCC: $19.00 
Published on Web 03/03/2000

The thermodynamic sink represented by the mineral forms of manganese and iron often limits the utility, especially in aqueous media, of functional catalysts based on common ligands such as polyamines and polyethers.[13] *N*,*N*′,*N*″-Trimethyl-1,4,7-triazacyclononane, $Me_3$[9]aneN3, provides an example in which manganese and iron complexes retain some solubility and the manganese complex is a potent oxidation catalyst.[14] A principal feature of this and other significant catalysts having common nitrogen donors and vacant coordination sites is their tendency to form dimers in which higher valent metal ions are present.

We hypothesized that the principles of modern coordination chemistry[15] should allow us to design ligands that would be strikingly resistant to oxidative hydrolysis while still having available sites for direct binding of the metal ion to either or both a terminal oxidant and/or substrate. The importance of having two cis labile sites (as in the complexes of **1** and **2**) has been discussed in relation to various catalytic and biomimetic processes.[16] We propose that the optimum number of available sites may be two, since this would facilitate a decrease in coordination number at the higher oxidation level; i.e., a diaqua complex of manganese(II) could transform into an oxo complex of manganese(IV). Such a transformation would require adjacent coordination sites. Further, since the lower oxidation state species, manganese(II) and iron(II), are commonly 6-coordinate, tetradentate ligands are preferred. The obvious ligand to satisfy these relationships is 1,4,7,10-tetraazacyclododecane, often labeled *cyclen*, or, systematically, [12]aneN4. It binds to first row transition ions exclusively in a folded conformation because its internal cavity is too small to encompass those metal ions. With the tetraaza macrocyclic ligand in such a conformation, the remaining two metal ion sites are, of course, adjacent to each other (cis). The principal limitation of cyclen in such catalytic roles arises because of its folded conformation. It has been well demonstrated with other macrocyclic complexes that the folded form gives up its metal ion much more rapidly than do planar macrocycles.[17] These considerations led to the ligands used in the studies reported here.

It is well-known today that, given good complementarity and the same donor atoms, both the thermodynamic and kinetic stabilities of metal complexes increase in the series monodentate ligand < linear or branched chelating ligand < macrocyclic ligand < macrobicyclic ligand, or cryptate. This sequence may be stated simply as follows: given equal complementarity, complex stability increases with the topological complexity of the ligand as recognized in the chelate effect, the macrocyclic effect, and the cryptate effect.[15] Now, we wanted to retain the features that cyclen would produce in an octahedral complex while achieving a level of stability comparable to the strongest

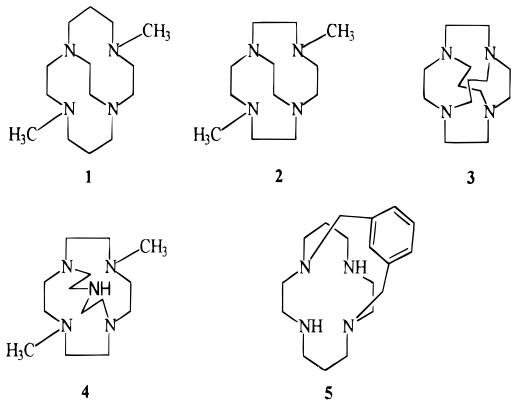


**Figure 1.** Recently reported cross-bridged ligands (for **1**−**5**, see refs 18a−e, respectively).

complexes, for example, that of such bicyclic ligands as cryptates. To do this we required a tetradentate ligand that is as topologically constrained as the macrobicyclic cryptates. This led us to postulate cross-bridged tetraazamacrocycles (Figure 1, structures **1**−**5**).[18] Consultation of the literature soon revealed that these special organic molecules had already been synthesized in other laboratories, but that they had not been fully exploited as transition metal ligands. Also, their proton-sponge nature presented a great challenge to the synthesis of all but the strongest binding transition metal ions (i.e., $Cu^{2+}$ and $Ni^{2+}$).[19] We proposed that the great rigidity of these short cross-bridged ligands, especially ethylene-bridged **1** and **2**, should impart enormous kinetic stability to their complexes,[15] and we have recently shown this to be the case for $Cu^{2+}$.[20] This kinetic stability confers on these transition metal complexes great promise in such applications as homogeneous catalysis, where complex stability has historically been a problem.

With full recognition of the potential of these systems, we began a program aimed at broadening the range of metal complexes of the ethylene cross-bridged tetraazamacrocycles initially reported by Weisman et al. (**1**)[18a] and Bencini et al. (**2**).[18b] Attracted by the expectation of greatly diminished kinetic lability and enhanced thermodynamically stability, our goals have been to develop synthetic methods for the introduction of metal ions into the highly basic ligand cleft and to explore the capabilities of the resulting complexes for biomimetic and catalytic applications. We report here methods for synthesizing the $Fe^{2+}$ and $Mn^{2+}$ complexes with two topologically constrained cross-bridged tetraazamacrocycles, **1** and **2**, the exciting chemical and physical properties of the new complexes, their X-ray crystal structures, and catalytic activity in oxidation reactions.

## Experimental Section

*N*,*N*′-Bis(aminopropyl)ethylenediamine (98%) was purchased from Acros Organics. Glyoxal (40 wt % in water), methyl iodide (99%), and sodium borohydride (98%) were purchased from Aldrich Chemical

(13) Cotton, F. A.; Wilkinson, G. *Advanced Inorganic Chemistry*, 5th ed.; Wiley & Sons: New York, 1988.

(14) (a) Wieghardt, K.; Bossek, U.; Nuber, B.; Weiss, J.; Bonvoisin, J.; Corbella, M.; Vitols, S. E.; Girerd, J. J. *J. Am. Chem. Soc.* **1988**, *110*, 7398. (b) Quee-Smith, V. C.; DelPizzo, L.; Jurellar, S. H.; Kershner, J. L.; Hage, R. *Inorg. Chem.* **1996**, *35*, 6461. (c) Koek, J. H.; Russel, S. W.; van der Wolf, L.; Hage, R.; Warnaar, J. B.; Spek, A. L.; Kershner, J.; DelPizzo, L. *J. Chem. Soc., Dalton Trans*. **1996**, 353. (d) De Vos, D. E.; Bein, T. *J. Organomet. Chem.* **1996**, *520*, 195.

(15) Busch, D. H. *Chem. Rev.* **1993**, *93*, 847.

(16) (a) Alexander, M. D.; Busch, D. H. *J. Am. Chem. Soc.* **1966**, *88*, 1130. (b) Chin, J.; Banaszczyk, M.; Jubian, V.; Zou, X. *J. Am. Chem. Soc.* **1989**, *111*, 186. (c) Hettich, R.; Schneider, H.-J. *J. Am. Chem. Soc.* **1997**, *119*, 5638. (d) Arciero, D. M.; Lipscomb, J. D. *J. Biol. Chem.* **1986**, *261*, 2170. (e) Halfen, J. A.; Mahapatra, S.; Wilkinson, E. C.; Kaderli, S.; Young, V. G., Jr.; Que, L., Jr.; Zuberbühler, A. D.; Tolman, W. B. *Science* **1996**, *271*, 1397. (f) Ross, P. K.; Solomon, E. I. *J. Am. Chem. Soc.* **1991**, *113*, 3246.

(17) (a) Cabiness, D. K.; Margerum, D. W. *J. Am. Chem. Soc.* **1970**, *92*, 2151. (b) Lindoy, L. F. *The Chemistry of Macrocyclic Ligand Complexes*; Cambridge University Press: Cambridge, 1989; p 186.

(18) (a) Weisman, G. R.; Rogers, M. E.; Wong, E. H.; Jasinski, J. P.; Paight, E. S. *J. Am. Chem. Soc.* **1990**, *112*, 8604. (b) Bencini, A.; Bianchi, A.; Bazzicalupi, C.; Ciampolini, M.; Fusi, V.; Micheloni, M.; Nardi, N.; Paoli, P.; Valtancoli, B. *Supramol. Chem.* **1994**, *3*, 41. (c) Springborg, J.; Olsen, C. E.; Søtofte, I. *Acta Chem. Scand.* **1995**, *49*, 555. (d) Dapporto, P.; Paoli, P.; Bazzicalupi, C.; Bencini, A.; Nardi, N.; Valtoncoli, B.; Fusi, V. *Supramol. Chem.* **1996**, *7*, 195. (e) Denat, F.; Lacour, S.; Brandes, S.; Guilard, R. *Tetrahedron Lett.* **1997**, *38*, 4417.

(19) (a) Weisman, G. R.; Wong, E. H.; Hill, D. C.; Rogers, M. E.; Reed, D. P.; Calabrese, J. C. *J. Chem. Soc., Chem. Commun.* **1996**, 947. (b) Irving, H.; Williams, R. J. P. *J. Chem. Soc.* **1953**, *Part III*, 3192.

(20) Hubin, T. J.; McCormick, J. M.; Collinson, S. R.; Alcock, N. W.; Busch, D. H. *J. Chem. Soc., Chem. Commun.* **1998**, 1675.

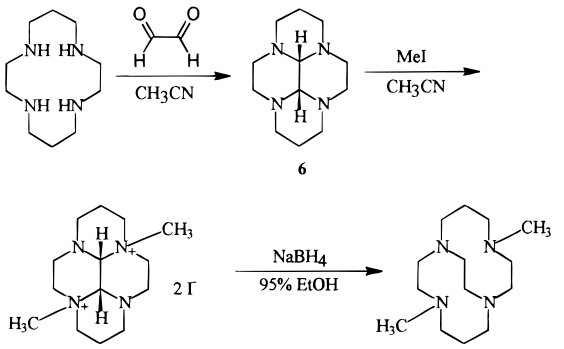


**Figure 2.** The literature procedure[19a] for the synthesis of cross-bridged macrocycles exploits the cis fusion of the tetracyclic structure **6** to selectively alkylate at nonadjacent sites, which facilitates ring-opening reduction to form the desired cross-bridged ligand.

Co. Cyclen was generously supplied by Dow Chemical Co. All solvents were of reagent grade and were dried, when necessary, by accepted procedures.[21]

Elemental analyses were performed by the Analytical Service of the University of Kansas or Desert Analytics. Mass spectra were measured by the Analytical Service of the University of Kansas on a VG ZAB HS spectrometer equipped with a xenon gun. Matrices used include NBA (nitrobenzyl alcohol) and TG/G (thioglycerol-glycerol). NMR spectra were obtained on a Bruker AM-500 spectrometer.

**Synthesis.** 4,11-Dimethyl-1,4,8,11-tetraazabicyclo[6.6.2]hexadecane (**1**) and 4,10-dimethyl-1,4,7,10-tetraazabicyclo[5.5.2]tetradecane (**2**) were prepared according to literature procedures from cyclam,[18a] which was made from *N*,*N*′-bis(aminopropyl)ethylenediamine using a modified literature procedure,[22] and from cyclen,[19a] which was obtained from Dow (see Figure 2). A further study of the organic synthesis of **1**, including structural characterization of various precursors, was conducted in our labs and is described elsewhere.[23]

**(a) 4,11-Dimethyl-1,4,8,11-tetraazabicyclo[6.6.2]hexadecane Bis-(trifluoroacetate)**. To 510 mg (2.00 mmol) of **1** dissolved in 25 mL of dry methanol in an ice bath was added 5 mL of trifluoroacetic acid (TFA) dissolved in 15 mL of dry methanol, dropwise at first and then in larger portions. After the addition was complete, the reaction was stirred under ice cooling for ~15 min. The methanol and excess TFA were removed under vacuum to give an oil, which was solidified by addition of dry ether and stirring for several minutes. The solid was recovered by filtration, washed copiously with dry ether, and partially dried on the frit. Further drying of the solid was accomplished under vacuum. The crude ligand salt was recrystallized from dry methanol by addition of dry ether to the onset of turbidity and cooling in a freezer. Filtration of the resulting solid, washing with dry ether, and drying gave 700 mg (73%) of an off-white solid. Anal. Calcd for $C_{16}H_{32}N_4O_4F_6$ C 44.8, H 6.7, and N 11.61, found C 45.1, H 7.1, and N 11.58. The NMR in $D_2O$ and the EI mass spectrum in methanol of the ligand salt were nearly identical with that of the free ligand.[23]

**(b) $MLCl_2$ (M = $Mn^{2+}$, $Fe^{2+}$; L = 1, 2)**. The ligand (1 mmol) was dissolved in 15 mL of dry $CH_3CN$ in a 25 mL Erlenmeyer flask in an inert atmosphere glovebox. A suspension of 1 mmol of $M(py)_2Cl_2$ (M = $Fe^{2+}$, $Mn^{2+}$), synthesized by literature procedures,[24] in 5 mL of acetonitrile was added to the stirring ligand solution. After approximately 2 h, all of the metal salt had dissolved. The reaction was stirred for an additional 12−14 h, then filtered. The colorless ($Mn^{2+}$) or tan ($Fe^{2+}$) filtrates were allowed to evaporate under nitrogen, yielding large pale blue-green ($Mn^{2+}$) or tan ($Fe^{2+}$) crystals suitable for X-ray diffraction. Yield: 69−85%. Fe(**1**)$Cl_2$: Anal. Calcd for $C_{14}H_{30}N_4FeCl_2$ C 44.11, H 7.93, and N 14.70, found C 44.08, H 8.00, and N 15.00. Mn(**1**)$Cl_2$: Anal. Calcd for $C_{14}H_{30}N_4MnCl_2$ C 44.22, H 7.95, and N 14.73, found C 44.39, H 8.13, and N 14.81. Fe(**2**)$Cl_2$: Anal. Calcd for $C_{12}H_{26}N_4FeCl_2$ C 40.82, H 7.42, and N 15.87, found C 40.51, H 7.52, and N 15.57. Mn(**2**)$Cl_2$: Anal. Calcd for $C_{12}H_{26}N_4MnCl_2$ C 40.92, H 7.44, and N 15.91, found C 41.14, H 7.41, and N 15.99. $FAB^+$ mass spectra in acetonitrile (NBA matrix) exhibited peaks at *m*/*z* $MLCl^+$ for all complexes. [An alternative synthesis using anhydrous $MCl_2$ can be found in ref 25.]

**Physical Methods.** Electrochemical experiments were performed on a Princeton Applied Research Model 175 programmer and Model 173 potentiostat in dry $CH_3CN$ using a homemade cell in an inert atmosphere drybox under $N_2$. Either a button Pt or a button glassy carbon electrode was used as the working electrode in conjunction with a Pt-wire counter electrode and a Ag-wire pseudo-reference electrode. Tetrabutylammonium hexafluorophosphate (0.1 M) was the supporting electrolyte in all cases. The measured potentials were referenced to SHE using ferrocene (+0.400 V versus SHE) as an internal standard.

EPR spectra were recorded on a Bruker ESP300E spectrometer operating in the X-band using ~1 mM complex in dry ethanol at 77 K. Electronic spectra were recorded using a Cary 3 spectrometer controlled by a Dell Dimension XPS P133s computer.

Magnetic studies were performed on a previously described force magnetometer with an external magnetic field of 5 kG in the temperature range 5−295 K.[26] The samples were pumped for over 3 h under a vacuum of 50 mTorr before the sample chamber was filled with helium gas for variable-temperature measurements.

Conductance measurements[27] were obtained with a YSI Model 35 conductance meter at room temperature. The molar conductances of the complexes were determined from readings at several dilutions and extrapolated to $\Lambda_o$. An Onsager plot[27b] for the complexes in each solvent was constructed to confirm the electrolyte type.

Potentiometric titrations were performed under $N_2$ at 25.0 °C with an ionic strength of 0.1000 ($KNO_3$) on a Brinkmann Metrohm 736GP Titrino equipped with a Brinkmann combination electrode. The electrode was standardized by a five buffer calibration using Titrino's internal standardization method followed by titration of a standardized strong acid ($HNO_3$) with a standardized strong base (KOH) after a literature procedure.[28] The strong acid and the strong base solutions were prepared from carbonate-free water and standardized with Titrino's internal methods. The KOH solution was stored under $N_2$ to minimize carbonate formation. In a typical titration ~10 mg of the material to be titrated was placed in 50.0 mL of the supporting electrolyte solution and ~2 mL of the $HNO_3$ solution was added to a $p[H^+] < \sim 3$. The resulting solution was titrated to a $p[H^+]$ value between 11 and 12. The data were fit using the program BETA,[29] which is an updated version of a previous program of the same name,[30] using the $pK_w$ found in the strong acid/base titration. For **1** five replicate titrations were performed each with a goodness of fit (GOF)[28] < 2.2 and a total of 1194 data points. Six replicate titrations (1791 data points total) each with a GOF < 2.4 were performed to determine the $pK_a$ of Mn(**1**)$Cl_2$.

**Crystal Structure Analysis.** X-ray data were collected with a Siemens SMART[31] three-circle system with CCD area detector using graphite monochromated Mo K radiation ($l$ = 0.71073 Å). The crystals were held at the specified temperature with the Oxford Cryosystem

(21) Perrin, D. D.; Armarego, W. L. F.; Perrin, D. R. *Purification of Laboratory Chemicals*, 2nd ed.; Pergamon Press: New York, 1980.

(22) Barefield, E. K.; Wagner, F.; Herlinger, A. W.; Dahl, A. R. *Inorg. Synth.* **1976**, *16*, 220.

(23) Hubin, T. J.; McCormick, J. M.; Alcock, N. W.; Busch, D. H. **1998**, manuscript in preparation.

(24) Witteveen, H. T.; Nieuwenhuijse, B.; Reedijk, J. *J. Inorg. Nucl. Chem.* **1974**, *36*, 1535.

(25) (a) Busch, D. H.; Collinson, S. R.; Hubin, T. J. *Catalysts and Methods for Catalytic Oxidation*, WO 98/39098, Sept. 11, 1998. (b) Busch, D. H.; Collinson, S. R.; Hubin, T. J.; Labeque, R.; Williams, B. K.; Johnston, J. P.; Kitko, D. J.; Burkett-St. Laurent, J. C. T. R.; Perkins, C. M. *Bleach Compositions*, WO 98/39406, Sept. 11, 1998.

(26) Kahol, P. K.; McCormick, B. J. *J. Phys.: Condens. Matter*. **1991**, *3*, 7963.

(27) (a) Angelici, R. J. *Synthesis and Techniques in Inorganic Chemistry*; University Science Books: Mill Valley, CA, 1986; Appendix 2. (b) Feltham, R. D.; Hayter, R. G. *J. Chem. Soc.* **1964**, 4587. (c) Geary, W. J. *Coord. Chem. Rev.* **1971**, *7*, 81.

(28) Turowski, P. N.; Rodgers, S. J.; Scarrow, R. C.; Raymond, K. N. *Inorg. Chem.* **1988**, *27*, 474.

(29) McCormick, J. M.; Raymond, K. N. Unpublished results.

(30) (a) Avdeef, A.; Raymond, K. N. *Inorg. Chem.* **1979**, *18*, 1605. (b) Harris, W. R.; Raymond, K. N. *J. Am. Chem. Soc.* **1979**, *101*, 6534.

(31) SMART User's manual, Siemens Industrial Automation Inc, Madison, Wisconsin.

**Table 1.** Crystal Data and Structural Refinement Details

| | Mn(**1**)$Cl_2$ | Fe(**1**)$Cl_2$ | Mn(**2**)$Cl_2$ | Fe(**2**)$Cl_2$ |
|---|---|---|---|---|
| formula | $MnC_{14}H_{30}N_4Cl_2$ | $FeC_{14}H_{30}N_4Cl_2$ | $MnC_{12}H_{26}N_4Cl_2$ | $FeC_{12}H_{26}N_4Cl_2$ |
| formula weight | 380.26 | 381.17 | 352.21 | 353.12 |
| crystal system | monoclinic | monoclinic | monoclinic | monoclinic |
| space group | $P2_1/c$ | $P2_1/c$ | $P2_1/c$ | $P2_1/c$ |
| $a$ (Å) | 8.297(1) | 8.2569(5) | 16.056(2) | 16.000(2) |
| $b$ (Å) | 13.919(2) | 13.794(1) | 13.543(2) | 13.482(1) |
| $c$ (Å) | 15.901(2) | 15.849(1) | 15.206(2) | 15.076(2) |
| $\beta$ (deg) | 100.621(5) | 101.077(5) | 102.129(5) | 102.669(5) |
| $V$ (Å$^3$) | 1804.87(9) | 1771.43(4) | 3232.56(14) | 3172.86(10) |
| $Z$ | 4 | 4 | 8 | 8 |
| $\rho_{calc}$ (g/cm$^3$) | 1.399 | 1.429 | 1.447 | 1.478 |
| temp (K) | 220(2) | 180(2) | 230(2) | 180(2) |
| abs coeff (cm$^{-1}$) | 10.27 | 11.53 | 11.41 | 12.81 |
| crystal size (mm) | 0.38 × 0.20 × 0.18 | 0.38 × 0.20 × 0.18 | 0.38 × 0.20 × 0.18 | 0.38 × 0.20 × 0.18 |
| $\theta$ range (deg) | 1.96−28.35 | 1.97−28.56 | 1.30−24.00 | 2.00−28.58 |
| index ranges | $-11 \le h \le 10$ | $-9 \le h \le 10$ | $-15 \le h \le 20$ | $-15 \le h \le 21$ |
| | $-18 \le k \le 18$ | $-15 \le k \le 18$ | $-15 \le k \le 17$ | $-15 \le k \le 17$ |
| | $-10 \le l \le 20$ | $-20 \le l \le 20$ | $-20 \le l \le 20$ | $-19 \le l \le 19$ |
| no. of reflns collected | 10463 | 10757 | 14978 | 18814 |
| no. of independent reflns | 4145 | 4140 | 5058 | 7435 |
| no. of obsd reflns[a] | 2710 | 3822 | 3253 | 5342 |
| refinement method | full-matrix on $F^2$ | full-matrix on $F^2$ | full-matrix on $F^2$ | full-matrix on $F^2$ |
| data/parameters | 4145/192 | 4140/190 | 5058/347 | 7435/348 |
| goodness of fit on $F^2$ | 1.133 | 1.069 | 1.123 | 1.015 |
| final $R$ indices[a] | $R1 = 0.0819$ | $R1 = 0.0317$ | $R1 = 0.0612$ | $R1 = 0.0361$ |
| | $wR2 = 0.1875$ | $wR2 = 0.0703$ | $wR2 = 0.1122$ | $wR2 = 0.0729$ |
| $R$ indices (all data)[b,c] | $R1 = 0.1330$ | $R1 = 0.0377$ | $R1 = 0.1144$ | $R1 = 0.0621$ |
| | $wR2 = 0.2228$ | $wR2 = 0.0728$ | $wR2 = 0.1390$ | $wR2 = 0.0815$ |
| wt parameters $a$, $b$ | 0.0884, 3.8651 | 0.0258, 1.1975 | 0.0301, 8.9522 | 0.0320, 0.8800 |
| largest peak/hole (eÅ$^{-3}$) | 1.153 and −1.259 | 0.403 and −0.638 | 0.436 and −0.385 | 0.501 and −0.466 |

[a] $[I > 2\sigma(I)]$. [b] $wR1 = \sum||F_o| - |F_c||/|F_o|$. [c] $wR2 = \{\sum[w(F_o^2 - F_c^2)^2]/\sum[w(F_o^2)^2]\}^{1/2}$. Calculated $w = 1/[\sigma^2(F_o^2) + (aP)^2 + bP]$ where $P = (F_o^2 + 2F_c^2)/3$.

Cooler.[32] Absorption corrections were applied by the Ψ-scan method, and none of the crystals showed any decay during data collection. The Mn(**1**)$Cl_2$ crystals were of poor quality giving weak diffraction and a corresponding relatively high final $R$-value and Fourier residuals. For Fe(**2**)$Cl_2$ an extinction correction was applied, coefficient 0.00141(15). Complete data for all crystal are shown in Table 1.

Systematic absences indicated that the space group was $P2_1/c$ for all the compounds. The structures were solved by direct methods using SHELXS[33] (TREF) with additional light atoms found by Fourier methods. Hydrogen atoms were added at calculated positions and refined using a riding model. Anisotropic displacement parameters were used for all non-H atoms, while H-atoms were given isotropic displacement parameters equal to 1.2 (or 1.5 for methyl hydrogen atoms) times the equivalent isotropic displacement parameter for the atom to which the H-atom is attached. Refinement used SHELXL 96.[34] Selected bond lengths and angles for the four complexes may be found in Table 2, while atomic coordinates for Mn(**1**)$Cl_2$, Fe(**1**)$Cl_2$, Mn(**2**)$Cl_2$, and Fe(**2**)$Cl_2$, respectively, may be found in the Supporting Information.

**General Catalytic Procedures.** Catalytic reactions were performed according to the following procedures: Stock solutions of 10 mM carbamazepine (Aldrich) in methanol and 40 mM Mn(**1**) in water have been prepared and appropriate aliquots (as stated in text) have been used for the reaction mixtures. 1,4-Cyclohexadiene (Aldrich) was used directly as received. Solvent compositions have been adjusted to the desired 1:1 ratio of MeOH and $H_2O$, TRIS buffer (pH 7), or carbonate buffer (pH 10). Into 5 mL of total reaction volume appropriate amounts of oxidizing agent have been added to initiate the reaction. Parallel experiments in the absence of catalyst were carrried out as a control. Quantitative analysis before the initiation of the reaction and of the reaction products were performed by HPLC. The carbamazepine and its epoxide and diol derivatives were separated on a Waters μBondapack $C_{18}$ column, eluted with a MeOH/$H_2O$ (1:1 v/v) mobile phase, flow rate of 1 mL/min, with retention times of 11.4, 6, and 4.9 min, respectively. UV−visible detection was at 210 nm. The 1,4-cyclohexadiene and benzene were eluted on the same column with a MeOH/$H_2O$ (3:2 v/v) mobile phase, detected at 215 nm at retention times of 6.2 and 4.1 min, respectively. The identification of the products was obtained by LC-MS analysis and by comparison of retention times with those of authentic samples.

(32) Cosier, J.; Glazer, A. M. *J. Appl. Crystallogr.* **1986**, *19*, 105.
(33) Sheldrick, G. M. *Acta Crystallogr.* **1990**, *A46*, 467.
(34) Sheldrick, G. M, SHELX-96 (beta-test) (including SHELXS and SHELXL), University of Göttingen, 1996.

## Results and Discussion

**Preparation of Metal Complexes.** In synthetic chemistry, large gains are usually achieved by overcoming substantial challenges, and that is certainly the case here. As noted above and in a previous communication,[20] only $Cu^{2+}$ and $Ni^{2+}$, the thermodynamically strongest binding (first row, divalent) transition metal ions, had been complexed to ethylene cross-bridged tetraazamacrocycles prior to our work.[19] Our attempts at the complexation of **1** and **2** with $Fe^{2+}$ and $Mn^{2+}$ salts in protic solvents or in aprotic solvents using hydrated metal salts were entirely unsuccessful. We therefore soon concluded that $Cu^{2+}$ and $Ni^{2+}$ are much better at competing with protons for the binding cavity in protic solvents than most divalent transition metal ions. This is especially true of the ions of primary interest here, the relatively "hard" oxyphilic ions of manganese and iron.

We attribute this behavior to the proton-sponge nature of the ligands. Weisman et al. studied the protonation of **1** by NMR techniques, reporting $pK_{a2} > 24$ and $pK_{a1} = 10.8$.[18a] We have confirmed the latter value by titration in an aqueous medium (Figure 3). In water, the diprotonated form of free ligand **1** behaves as a monoprotic weak acid with a $pK_{a1}$ of 9.58(3) even though stoichiometrically there are two $H^+$ bound, indicating the $pK_{a2}$ must be substantially greater than 13. The difference between the value for $pK_{a1}$ from our measurements and that from the previous study probably arises from the different solvents and methods used. This difference does not change the conclusion that these ligands bind at least one proton very,

**Table 2.** Selected Bond Lengths (Å) and Angles (deg)

| | | | | | | | |
|---|---|---|---|---|---|---|---|
| | | | | (i) For Mn(**1**)$Cl_2$: | | | |
| Mn(1)−N(3) | 2.325(4) | Mn(1)−N(1) | 2.347(4) | N(3)−Mn(1)−N(2) | 79.52(14) | N(4)−Mn(1)−Cl(3) | 99.89(11) |
| Mn(1)−N(2) | 2.332(4) | Mn(1)−Cl(3) | 2.455(2) | N(3)−Mn(1)−N(4) | 158.0(2) | N(1)−Mn(1)−Cl(3) | 93.55(12) |
| Mn(1)−N(4) | 2.333(4) | Mn(1)−Cl(2) | 2.456(2) | N(2)−Mn(1)−N(4) | 83.45(14) | N(3)−Mn(1)−Cl(2) | 100.05(11) |
| | | | | N(3)−Mn(1)−N(1) | 83.21(14) | N(2)−Mn(1)−Cl(2) | 92.42(11) |
| | | | | N(2)−Mn(1)−N(1) | 75.6(2) | N(4)−Mn(1)−Cl(2) | 94.42(12) |
| | | | | N(4)−Mn(1)−N(1) | 79.2(2) | N(1)−Mn(1)−Cl(2) | 166.88(11) |
| | | | | N(3)−Mn(1)−Cl(3) | 94.16(11) | Cl(3)−Mn(1)−Cl(2) | 98.85(6) |
| | | | | N(2)−Mn(1)−Cl(3) | 167.92(11) | | |
| | | | | (ii) For Fe(**1**)$Cl_2$: | | | |
| Fe(1)−N(1) | 2.2574(13) | Fe(1)−N(3) | 2.2866(14) | N(1)−Fe(1)−N(2) | 78.36(5) | N(4)−Fe(1)−Cl(3) | 100.14(4) |
| Fe(1)−N(2) | 2.2634(13) | Fe(1)−Cl(3) | 2.4260(5) | N(1)−Fe(1)−N(4) | 81.29(5) | N(3)−Fe(1)−Cl(3) | 92.13(4) |
| Fe(1)−N(4) | 2.2748(13) | Fe(1)−Cl(5) | 2.4273(4) | N(2)−Fe(1)−N(4) | 84.95(5) | N(1)−Fe(1)−Cl(5) | 170.07(4) |
| | | | | N(1)−Fe(1)−N(3) | 84.86(5) | N(2)−Fe(1)−Cl(5) | 93.87(4) |
| | | | | N(2)−Fe(1)−N(3) | 80.84(5) | N(4)−Fe(1)−Cl(5) | 91.95(4) |
| | | | | N(4)−Fe(1)−N(3) | 161.88(5) | N(3)−Fe(1)−Cl(5) | 100.14(4) |
| | | | | N(1)−Fe(1)−Cl(3) | 92.83(4) | Cl(3)−Fe(1)−Cl(5) | 95.53(2) |
| | | | | N(2)−Fe(1)−Cl(3) | 169.13(4) | | |
| | | | | (iii) For Mn(**2**)$Cl_2$: | | | |
| Mn(1)−N(11) | 2.313(5) | Mn(2)−N(25) | 2.312(5) | N(11)−Mn(1)−N(15) | 73.7(2) | N(25)−Mn(2)−N(21) | 74.5(2) |
| Mn(1)−N(15) | 2.315(5) | Mn(2)−N(21) | 2.318(5) | N(11)−Mn(1)−N(112) | 77.2(2) | N(25)−Mn(2)−N(212) | 74.7(2) |
| Mn(1)−N(112) | 2.318(5) | Mn(2)−N(212) | 2.321(4) | N(15)−Mn(1)−N(112) | 74.1(2) | N(21)−Mn(2)−N(212) | 75.3(2) |
| Mn(1)−N(18) | 2.331(5) | Mn(2)−N(28) | 2.333(5) | N(11)−Mn(1)−N(18) | 144.0(2) | N(25)−Mn(2)−N(28) | 75.2(2) |
| Mn(1)−Cl(1) | 2.421(2) | Mn(2)−Cl(21) | 2.430(2) | N(15)−Mn(1)−N(18) | 77.8(2) | N(21)−Mn(2)−N(28) | 142.0(2) |
| Mn(1)−Cl(2) | 2.434(2) | Mn(2)−Cl(22) | 2.441(2) | N(112)−Mn(1)−N(18) | 74.3(2) | N(212)−Mn(2)−N(28) | 75.0(2) |
| | | | | N(11)−Mn(1)−Cl(1) | 97.43(13) | N(25)−Mn(2)−Cl(21) | 94.33(13) |
| | | | | N(15)−Mn(1)−Cl(1) | 93.44(12 | N(21)−Mn(2)−Cl(21) | 100.85(13) |
| | | | | N(112)−Mn(1)−Cl(1) | 167.34(13) | N(212)−Mn(2)−Cl(21) | 168.92(13) |
| | | | | N(18)−Mn(1)−Cl(1) | 105.78(13) | N(28)−Mn(2)−Cl(21) | 103.77(13) |
| | | | | N(11)−Mn(1)−Cl(2) | 104.93(13) | N(25)−Mn(2)−Cl(22) | 169.24(13) |
| | | | | N(15)−Mn(1)−Cl(2) | 169.32(13) | N(21)−Mn(2)−Cl(22) | 104.31(13) |
| | | | | N(112)−Mn(1)−Cl(2) | 95.23(13) | N(212)−Mn(2)−Cl(22) | 94.64(12) |
| | | | | N(18)−Mn(1)−Cl(2) | 99.07(14) | N(28)−Mn(2)−Cl(22) | 101.23(14) |
| | | | | Cl(1)−Mn(1)−Cl(2) | 97.24(6) | Cl(21)−Mn(2)−Cl(22) | 96.39(7) |
| | | | | (iv) For Fe(**2**)$Cl_2$: | | | |
| Fe(1)−N(110) | 2.240(2) | Fe(2)−N(24) | 2.240(2) | N(110)−Fe(1)−N(14) | 77.31(7) | N(24)−Fe(2)−N(210) | 76.98(7) |
| Fe(1)−N(14) | 2.248(2) | Fe(2)−N(210) | 2.243(2) | N(110)−Fe(1)−N(11) | 76.15(7) | N(24)−Fe(2)−N(27) | 75.38(7) |
| Fe(1)−N(11) | 2.269(2) | Fe(2)−N(27) | 2.256(2) | N(14)−Fe(1)−N(11) | 76.96(7) | N(210)−Fe(2)−N(27) | 79.62(7) |
| Fe(1)−N(17) | 2.276(2) | Fe(2)−N(21) | 2.264(2) | N(110)−Fe(1)−N(17) | 77.04(7) | N(24)−Fe(2)−N(21) | 79.66(7) |
| Fe(1)−Cl(11) | 2.4071(6) | Fe(2)−Cl(21) | 2.3970(6) | N(14)−Fe(1)−N(17) | 76.74(7) | N(210)−Fe(2)−N(21) | 75.52(7) |
| Fe(1)−Cl(12) | 2.4161(7) | Fe(2)−Cl(22) | 2.4104(6) | N(11)−Fe(1)−N(17) | 145.78(7) | N(27)−Fe(2)−N(21) | 148.04(7) |
| | | | | N(110)−Fe(1)−Cl(11) | 94.44(5) | N(24)−Fe(2)−Cl(21) | 93.60(5) |
| | | | | N(14)−Fe(1)−Cl(11) | 171.63(5) | N(210)−Fe(2)−Cl(21) | 170.21(5) |
| | | | | N(11)−Fe(1)−Cl(11) | 99.87(5) | N(27)−Fe(2)−Cl(21) | 95.56(5) |
| | | | | N(17)−Fe(1)−Cl(11) | 103.03(5) | N(21)−Fe(2)−Cl(21) | 105.72(5) |
| | | | | N(110)−Fe(1)−Cl(12) | 172.06(5) | N(24)−Fe(2)−Cl(22) | 171.83(5) |
| | | | | N(14)−Fe(1)−Cl(12) | 94.86(5) | N(210)−Fe(2)−Cl(22) | 94.98(5) |
| | | | | N(11)−Fe(1)−Cl(12) | 103.59(5) | N(27)−Fe(2)−Cl(22) | 104.85(5) |
| | | | | N(17)−Fe(1)−Cl(12) | 100.07(5) | N(21)−Fe(2)−Cl(22) | 97.08(5) |
| | | | | Cl(11)−Fe(1)−Cl(12) | 93.42(2) | Cl(21)−Fe(2)−Cl(22) | 94.50(2) |

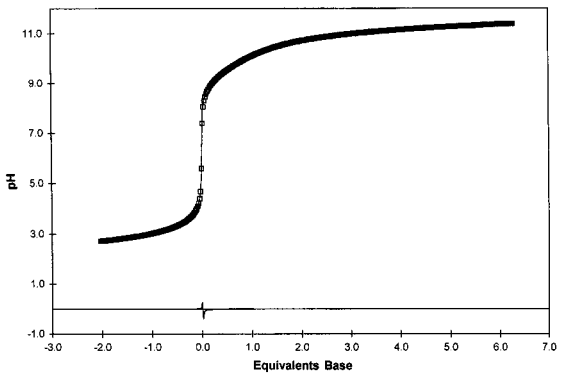


**Figure 3.** Titration data for **1** plotted against equivalents of base calculated per mole of **1**. The line through the data is the best fit as found by BETA and described in the text. The line near the baseline shows the residuals ($pH_{Obs} - pH_{Calc}$) for this fit.

very strongly, and that only the most strongly binding metal ions can compete with that proton for the cavity it occupies.

Having identified the obstacle, it was then rational to overcome it by minimizing the activity of protons in the reaction system. In our labs, the complexes of a broad array of transition metal ions have been prepared with these ligands only through the use of anhydrous metal reagents with strictly deprotonated ligands in rigorously dry, aprotic solvents under a dry, inert atmosphere.[20] The $Fe^{2+}$ and $Mn^{2+}$ complexes with ligands **1** and **2** were prepared from the corresponding anhydrous $M(py)_2Cl_2$ starting material in $CH_3CN$. Filtration to remove small amounts of insoluble contaminants followed by evaporation of the solvent yields pure complexes in all four cases.

**Crystal Structures.** X-ray crystal structures of the four complexes confirm the expected geometric properties and provide insight into the solution behavior of the new compounds. Figure 4 presents the crystal structures of Mn(**1**)$Cl_2$ and Fe(**2**)-$Cl_2$. The structures of Fe(**1**)$Cl_2$ and Mn(**2**)$Cl_2$ are visually identical with the structures shown, respective of the ligand, and are therefore not pictured here. As is the case for the two previously published structures of ethylene cross-bridged $Cu^{2+}$

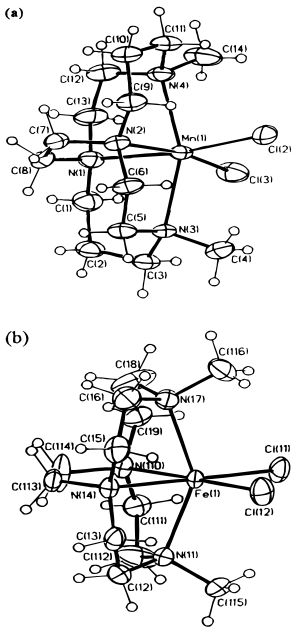


**Figure 4.** Views of the crystal structures of (a) Mn(**1**)$Cl_2$ and (b) Fe(**2**)$Cl_2$. The structures of Fe(**1**)$Cl_2$ and Mn(**2**)$Cl_2$ are visually identical with these complexes, respectively. Crystal data are given in Table 2, selected bond lengths and angles may be found in Table 3, and atomic coordinates are collected in Tables 4−7.

complexes[19a] (where the ligands are the *N*,*N*′-dibenzyl or *N*,*N*′-dihydro analogues of **1**), the ligands are found to be constrained to folded structures by the short cross-bridge. In all four cases, the macrobicycle occupies two axial and two cis equatorial sites of distorted octahedra, while the two chloride ligands occupy the remaining cis equatorial sites. These structures represent the first octahedral metal ions characterized for ligands of this class; the two previously published $Cu^{2+}$ structures involve pentacoordinate metal ions (although the benzyl derivative exhibits a sixth agostic interaction with a benzyl hydrogen). The structures of **2** also confirm that the smaller 12-membered-ring system behaves similarly to the 14-membered system of **1** and its analogues in transition metal coordination, contrary to an earlier report.[18b] In the chemistry of the unbridged parent macrocycles, with few exceptions,[35] 1,4,8,11-tetraazacyclotetradecane, or *cyclam*, binds metal ions in a square planar fashion,[36] occupying all four equatorial sites of octahedral complexes, which locates the two labile ligand binding sites at the trans, axial positions. Cyclen, as stated earlier, is too small to fit completely around the metal ion, and generally folds to occupy two cis equatorial and the two axial sites of octahedral metal ions,[37] a strict parallel to the coordination reported here for **1** and **2**. The short cross-bridge of **1** forces the cyclam ring system to behave more like cyclen. The consequences that two cis labile sites have on the reactivity of these complexes are currently being explored.[38]

A more detailed inspection of the four structures reveals several interesting trends. First, the size of the ring system dictates the distortion of the octahedra. The 14-membered ring in **1** engulfs the metal ion more fully than does the 12-membered ring in **2**. The two structures of **2** each contain two independent molecules per unit cell, although they both have nearly identical dimensions. The bond angles and lengths referred to below are taken from the arbitrarily assigned *first* molecule of each pair (see Table 2). The $N_{ax}-M-N_{ax}$ bond angle for Mn(**1**)$Cl_2$ is 158.0(2)°, while for Mn(**2**)$Cl_2$, it is only 144.0(2)°. Likewise, the $N_{eq}-M-N_{eq}$ angles are 75.6(2)° and 74.1(2)° for Mn(**1**)$Cl_2$ and Mn(**2**)$Cl_2$, respectively. The smaller angles for the smaller macrobicycle demostrate how the metal ion is less engulfed in the ligand cavity. The same trend is apparent in the $Fe^{2+}$ complexes: $N_{ax}-M-N_{ax}$ for Fe(**1**)$Cl_2$ is 161.88(5)°, while it is 145.78(7)° for Fe(**2**)$Cl_2$, and $N_{eq}-M-N_{eq}$ is 78.36(5)° for Fe(**1**)$Cl_2$ and 77.31(7)° for Fe(**2**)$Cl_2$.

A second broad observation is that the smaller $Fe^{2+}$ ion is more fully engulfed by both macrobicycles than is the larger $Mn^{2+}$ ion. $N_{ax}-M-N_{ax}$ is 161.88(5)° for Fe(**1**)$Cl_2$ while this angle is 158.0(2)° for Mn(**1**)$Cl_2$. The $N_{eq}-M-N_{eq}$ angles are 78.36(5)° and 75.6(2)° for Fe(**1**)$Cl_2$ and Mn(**1**)$Cl_2$, respectively. The same trend is seen with the ligand **2**: $N_{ax}-M-N_{ax}$ is 145.78(7)° for Fe(**2**)$Cl_2$ while this angle is 144.0(2)° for Mn(**2**)$Cl_2$ and the $N_{eq}-M-N_{eq}$ angles are 77.31(7)° and 74.1(2)° for Fe(**2**)$Cl_2$ and Mn(**2**)$Cl_2$, respectively.

Finally, in these closely related structures, the mutual orientations of the *N*-methyl groups are important. In all cases the *N*-methyl groups project above and below the plane containing the iron and two chlorides, an arrangement that may prevent dimerization by formation of M−O−M bridges. For both structures of ligand **1**, the methyl groups are "gauche", as viewed down the $N_{ax}-M-N_{ax}$ "axis" (Figure 5a). However, in the complexes of **2**, the same view shows that the *N*-methyl groups are "eclipsed" (Figure 5b). This phenomenon appears to be a result of the ligand size and symmetry. The larger **1** has two trimethylene chains and two ethylene chains connected to the methylated nitrogens. This asymmetry on the two sides of the methyl group seems to push it away from the trimethylene chain, resulting in the "gauche" alignment. The smaller ligand **2** is more symmetric, having only ethylene chains connected to the methylated nitrogens. With equivalent environments on each side then, the Me groups are not displaced from the expected "eclipsed" locations.

**Electronic Structure.** The result of most general interest is that the pseudo-octahedral metal ions in all four complexes are high spin with typical magnetic moments. Plots of experimental data in the forms $\chi T$ versus $T$ and $1/\chi$ versus $T$ (right-hand scale) are shown in Figure 6 for the representative compounds Mn(**1**)$Cl_2$ (Figure 6a) and Fe(**2**)$Cl_2$ (Figure 6b). The observed linear dependence of $1/\chi$ on temperature in both cases suggests that it is appropriate to treat the data with a modified Curie−Weiss model,

$$\chi = N\mu_{\text{eff}}{}^2/3k\,(T-\theta)$$

where $\chi$ is expressed per mole of manganese ions and $\theta$ is a Weiss-like constant to correct for the presence of interactions between neighboring complexes.

For the manganese complexes a linear regression of the $1/\chi$ versus $T$ data yields the $\mu_{\text{eff}}$ and $\theta$ values found in Table 3. The finite values for $\theta$ clearly indicate the presence of weak

(35) (a) Brewer, K. J.; Calvin, M.; Lumpkin, R. S.; Otvos, J. W.; Spreer, L. O. *Inorg. Chem.* **1989**, *28*, 4446. (b) Che, C.-M.; Kwong, S.-S.; Poon, C.-K.; Lai, T.-F.; Mak, T. C. W. *Inorg. Chem.* **1985**, *24*, 1359. (c) Poon. C.-K.; Che, C.-M. *J. Chem. Soc., Dalton Trans.* **1981**, 1336. (d) Lai, T.-F.; Poon, C.-K. *Inorg. Chem.* **1976**, *15*, 1562.

(36) (a) Fabbrizzi, L. *Comments Inorg. Chem.* **1985**, *4* (1), 33. (b) Martin, L. Y.; Sperati, C. R.; Busch, D. H. *J. Am. Chem. Soc.* **1977**, *99*, 2968. (c) Martin, L. Y.; Zompa, L. J.; DeHayes, L. J.; Busch, D. H. *J. Am. Chem. Soc.* **1974**, *96*, 4046.

(37) (a) Henrick, K.; Tasker, P. A.; Lindoy, L. F. *Prog. Inorg. Chem.* **1985**, *33*, 1. (b) Busch, D. H. *Acc. Chem. Res.* **1978**, *11*, 392. (c) Iitaka, Y. S.; Shina, M.; Kimura, E. *Inorg. Chem.* **1974**, *13*, 2886. (d) Collman, J. P.; Schneider, P. W. *Inorg. Chem.* **1966**, *5*, 1380.

(38) Buchalova, M.; Brockman, J. T.; Labeque, R.; Busch, D. H. Manuscript in preparation.

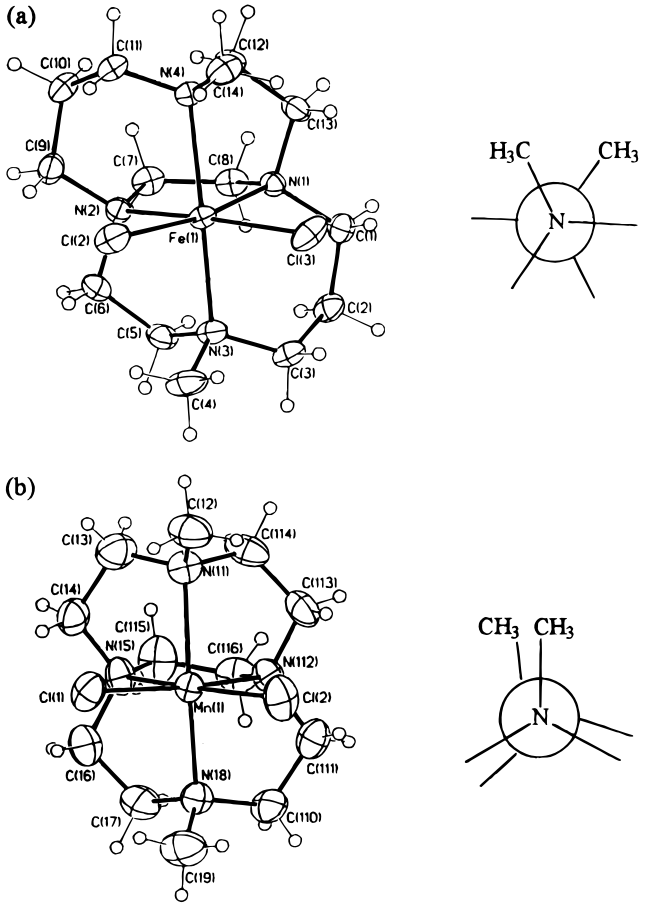


**Figure 5.** Representations of the crystal structures of (a) Fe(**1**)$Cl_2$ and (b) Mn(**2**)$Cl_2$ showing the "gauche" relationship of C4 and C14 in complexes of **1** and the "eclipsed" relationship of C12 and C19 in complexes of **2**. Beside each structure is a Newman projection down the $N_{ax}-M-N_{ax}$ axis to more clearly illustrate the conformational relationships.

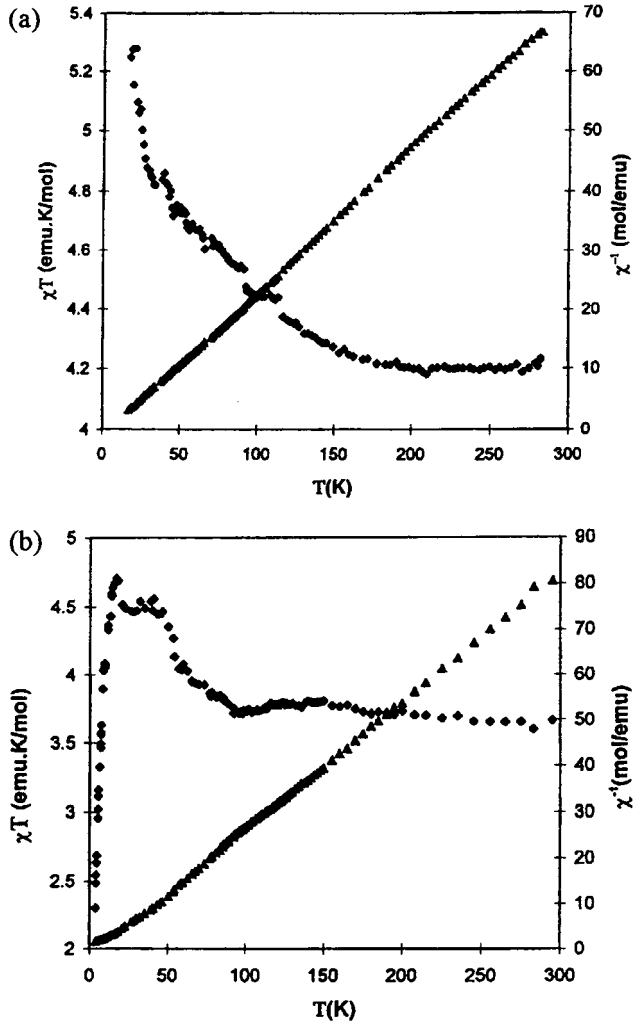


**Figure 6.** Magnetic data for (a) Mn(**1**)$Cl_2$ and (b) Fe(**2**)$Cl_2$.

**Table 3.** Magnetic Behavior of the Complexes

| complex | $\mu_{eff}$ ($\mu_B$) | $\theta$ ($cm^{-1}$) |
|---|---|---|
| Mn(**1**)$Cl_2$ | $5.80 \pm 0.06$ | $4.8 \pm 1.0$ |
| Mn(**2**)$Cl_2$ | $5.93 \pm 0.06$ | $2.4 \pm 0.9$ |
| Fe(**1**)$Cl_2$ | $5.50 \pm 0.02$ | $9.4 \pm 0.8$ |
| Fe(**2**)$Cl_2$ | $5.38 \pm 0.02$ | $3.2 \pm 0.5$ |
| | $\chi = N\mu_{eff}^2/3k_B(T-\theta)$ | |

ferromagnetic interactions between manganese ions. The experimetal data for the iron complexes show an increase of $\chi T$ with a decrease in temperature down to ~50 K, at which point a further decrease in temperature causes a reduction in $\chi T$. This behavior indicates the contribution of a significant single ion zero-field splitting, as expected for high-spin $Fe^{2+}$. Assuming that the single-ion effects are present only at low temperature, the data from 100 to 295 K were fit to the modified Curie−Weiss model, given above, to obtain the $\mu_{eff}$ and $\theta$ values found in Table 3 for the iron complexes.

The electronic spectra of these complexes, as exemplified by the two complexes of ligand **1**, and shown in Figure 7, have no intense absorption features in the UV−vis region except for a tailing absorbance at highest energy. However, the iron complexes exhibit a weak shoulder at about 350 nm that is not present in the corresponding manganese complexes. The absence of intense spectral features in this region is as expected for high-spin $d^5$ and $d^6$ complexes with ligands of this type.

The high-spin $d^5$ $Mn^{2+}$ complexes of **1** and **2** exhibit the expected six line EPR spectra in ethanol at 77 K, as shown in Figure 8. The signal is centered near $g = 2.00$ for both complexes and is consistent with the hyperfine splitting due to the coupling of the electron spin with the $I = {}^5/_2$ $^{55}Mn$ nucleus. The Mn(**2**)$Cl_2$ spectrum is much less well-behaved than that of Mn(**1**)$Cl_2$, yet six lines are still identifiable. The reason for this difference in the behavior of the two complexes is unknown. The $Fe^{2+}$ complexes are EPR silent at 77 K, as expected for high-spin $S = 2$ systems.

**Solution Properties.** The kinetic stability of these complexes under severe conditions is a matter of utmost importance. The dissociation of $Mn^{2+}$ from **1** in 1 M DCl was monitored by $^1H$ NMR by measuring the integrated intensity of the NMR spectrum of free ligand as a function of time. The protons on the metal complex are too paramagnetically broadened to be observed, but upon decomplexation the protons of the free ligand are observable, albeit broadened. In this way, the pseudo-first-order rate of dissociation in 1 M DCl was found (Figure 9) to be $1.4 \times 10^{-5}$ $s^{-1}$ ($t_{1/2} = 13.8$ h) at 298 K. Remarkably, this ligand dissociates from manganese(II) at a rate that is 12 orders of magnitude slower than the rate of water exchange from the hydrated manganese(II) ion. Other ligands, such as tetra(3-*N*-methylpyridyl)porphyrin,[39] dissociate with a half-life of 74 $\mu$s in 1 M HCl. Likewise, the addition of HCl or $HClO_4$ to an ethanol solution of the $Mn^{2+}$ complex of *meso*-5,5,7,12,12,14-

(39) Hambright, P. *Inorg. Nucl. Chem. Lett.* **1977**, *13*, 403.

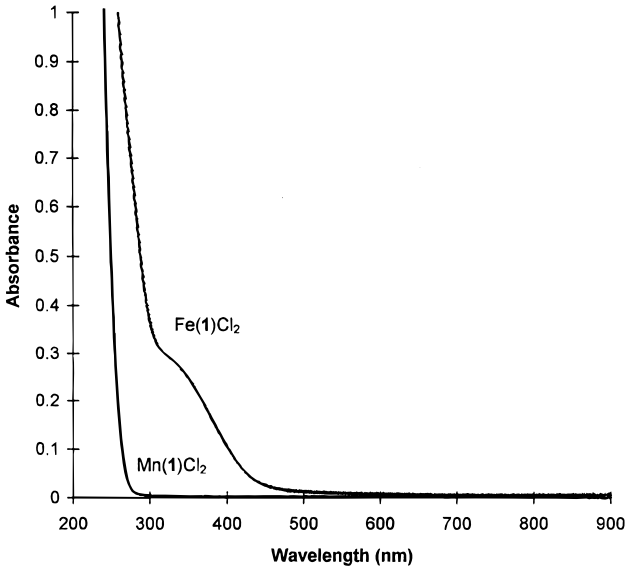


**Figure 7.** Electronic spectra of Mn(**1**)$Cl_2$ and Fe(**1**)$Cl_2$ in $CH_3CN$.

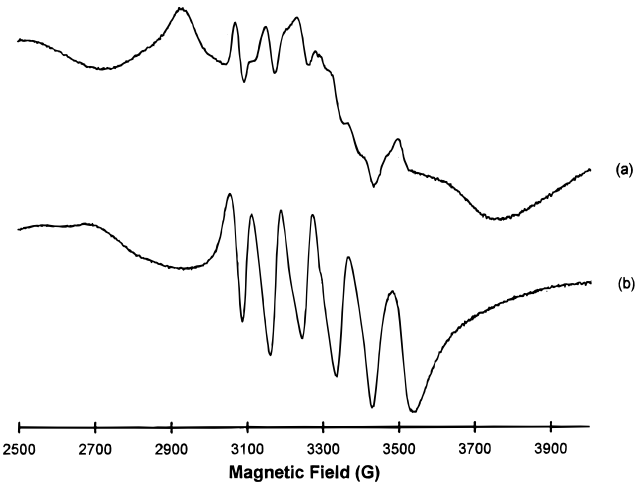


**Figure 8.** X-band EPR spectra of (a) Mn(**2**)$Cl_2$ and (b) Mn(**1**)$Cl_2$ (1 mM solutions in ethanol at 77 K).

hexamethyl-1,4,8,11-tetraazacyclotetradecane causes the instant precipitation of a white solid identified as the protonated ligand.[40] This complex does indeed enjoy, in relative terms, an immense increase in kinetic stability.

A comparison between the dissociation rate of ligand **1** from Mn(**1**)$(H_2O)_2^{2+}$ with the corresponding rate[20] for Cu(**1**)$(H_2O)^{2+}$ reflects fundamental relationships. The manganese complex, Mn(**1**)$(H_2O)_2^{2+}$, loses ligand **1** roughly 4000 times faster than copper(II) loses the same ligand. Further, the relative rates are more or less what one might expect on the basis of the complexing properties of the two metal ions. Soft copper(II) with its relatively great tendency to form covalent bonds should be more inert toward substitution than hard spherical manganese(II). This contrasts with the common knowledge that hydrated copper(II) and chromium(II) ions have the fastest water exchange rates from among the first row transition metal ions, whereas hydrated manganese(II) exchanges water at roughly an order of magnitude slower, a behavior attributed to a dynamic Jahn-Teller effect in the case of $Cu(H_2O)_6^{2+}$.

The titration data for Mn(**1**)$Cl_2$ (Figure 10) can be fit very well by treating the compound as a weak monoprotic acid. While the conductance measurements show that both chlorides are

(40) Bryan, P. S.; Dabrowiak, J. C. *Inorg. Chem.* **1975**, *2*, 296.

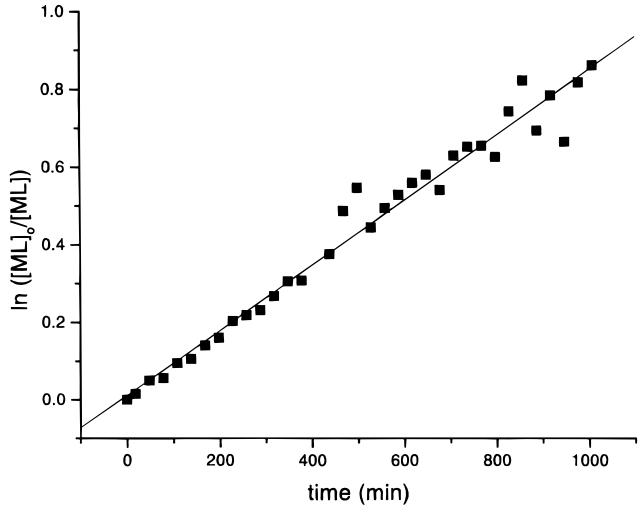


**Figure 9.** Kinetic data for the dissociation of Mn(**1**)$Cl_2$. The pseudo-first-order dissociation constant was calculated at $1.4 \times 10^{-5}$ $s^{-1}$ ($t_{1/2}$ = 13.8 h) for 0.1 M complex in 1 M DCl. (For the linear regression, $R^2 = 0.972$.)

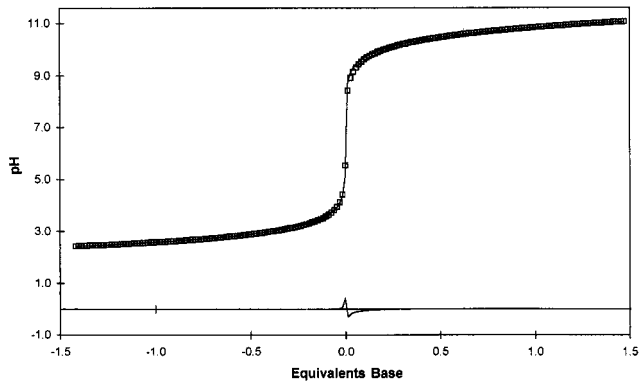


**Figure 10.** Titration data for Mn(**1**)$Cl_2$ plotted against equivalents of base calculated per mole of Mn(**1**)$Cl_2$. The line through the data is the best fit as found by BETA and described in the text. The line near the baseline shows the residuals ($pH_{Obs} - pH_{Calc}$) for this fit.

replaced by water in aqueous solution (vide infra), only one appears to have a p$K_a$ in the accessible p[$H^+$] region. The p$K_a$ for this bound water is 10.87(4), which agrees very well with that found for $Mn(H_2O)_6^{2+}$ (10.9)[41] and indicates that ligand **1** does not significantly alter the ability of $Mn^{2+}$ to polarize a water molecule from that of the hexaquo complex. This suggests that the combination of the tetradentate cross-bridged macrocycle and two water molecules leaves the electron density on the metal ion about the same as in the hydrated ion. We found this interesting because it follows that the great stability of the complex cannot be attributed to unusually strong bonds. In turn, this leads to the conclusion that the exceptional stability arises from topological and rigidity effects, and these were the relationships considered in the ligand design.

$Mn^{II}$ is a rather peculiar first-row transition metal ion and that peculiarity requires special ligands to control it, especially in aqueous solution. The high-spin $d^5$ electron configuration of $Mn^{II}$ in most of its complexes both produces an oversized spherical ion and virtually eliminates meaningful study of its complexes by electronic spectroscopy or conventional NMR. This explains the historical tendency to neglect the coordination chemistry of the metal ion prior to the onset of bioinorganic

(41) Martell, A. E.; Smith, R. M.; Motekaitis, R. J. *NIST Standard Reference Database 46, Version 2.0*; NIST Standard Reference Data: Gaithersberg, MD, 1995.

**Table 4.** Molar Conductances in Several Solvents

| | $\Lambda_o$(molar conductance) | | | | | | | |
|---|---|---|---|---|---|---|---|---|
| | nitromethane | | acetonitrile | | methanol | | water | |
| complex/ electrolyte type | $\Lambda_o$ | slope of Onsager plot | $\Lambda_o$ | slope of Onsager plot | $\Lambda_o$ | slope of Onsager plot | $\Lambda_o$ | slope of Onsager plot |
| Mn(**1**)$Cl_2$ | 0.72 | −2.57 | 8.70 | 36.4 | 95.0 | 288 | 205 | 100 |
| Fe(**1**)$Cl_2$ | *a* | *a* | 47.2 | 164 | 71.9 | 96.3 | 266 | 126 |
| Mn(**2**)$Cl_2$ | 1.17 | 5.54 | 29.4 | 158 | 85.6 | 230 | 245 | 115 |
| Fe(**2**)$Cl_2$ | *a* | *a* | 62.3 | 374 | 122.3 | 268 | 278 | 182 |
| | | | | Literature Values | | | | |
| 1:1[b] | 75−95 | 200 | 120−160 | NA | 80−115 | 256 | 118−131 | 92 |
| 2:1[b] | 150−180 | 465 | 220−300 | NA | 160−220 | 514 | 235−273 | 185 |

[a] Nitromethane reacted with Fe(**1**)$Cl_2$ and Fe(**2**)$Cl_2$. [b] See Reference 17.

chemistry. The spherical nature and early position in the Irving−Williams series[19b] of $Mn^{II}$ predict the observed lability and instability of its complexes. An added complication is the ease of which many $Mn^{II}$ complexes are oxidized by dioxygen, generally to insoluble $MnO_2$ in aqueous systems. As noted above, the p$K_a$ of $Mn(H_2O)_6^{2+}$ is also very high, higher than the corresponding Fe, Co, Ni, Cu, and Zn analogues.[41] The combination of these properties describes a metal ion that complexes common ligands only very weakly compared to most divalent transition metal ions. Considering this fact and the proton-sponge nature of the present ligands, it might have been viewed as unlikely that they could be united in complex formation. Yet by judicious application of the principles of the *compleat coordination chemistry*[15] these two apparently mismatched reagents can be teamed to produce exciting new complexes with valuable properties.

The results of conductance experiments (Table 4) reflect the ease with which the chloride ligands may be replaced by solvent. The ionization (displacement of chloride by solvent) of these complexes in solution correlates with the solvent dielectric constant. In low dielectric solvents, like nitromethane and acetonitrile, the complexes behave as nonelectrolytes revealing that the chlorides remain bound and indicating that the structure of the complex in solution is essentially as in the solid state (crystal structure).[42] In coordinating solvents with slightly higher dielectric constants, like methanol, all four complexes behave as 1:1 electrolytes which implies that solvent has displaced one chloride ligand from the coordination sphere while the second chloride remains bound. In water, 2:1 electrolyte behavior is exhibited for the complexes, indicating that both chlorides have been replaced by water molecules. The electrolyte type in aqueous media combines with the conclusions drawn above about substitution rates to predict that the complex will be capable of surviving in a catalysis medium for substantial periods of time and that the two available sites for binding of terminal oxidant and/or substrate are capable of undergoing substitution at rapid rates.

Electrochemical studies further confirm the promise of the manganese complex for homogeneous oxidative catalysis in aqueous media. The cyclic voltammograms of the complexes are shown in Figure 11 and the redox potentials and peak separations are given in Table 5. These rigid ligands stabilize a range of oxidation states for manganese, from $Mn^{2+}$ to $Mn^{4+}$ as shown by the two reversible oxidations of Mn(**1**)$Cl_2$ and Mn(**2**)$Cl_2$. In contrast, only the $Fe^{3+}/Fe^{2+}$ couple is observed for Fe(**1**)$Cl_2$ and Fe(**2**)$Cl_2$. From this perspective the manganese complexes are very likely to function as oxidation catalysts with a variety of terminal oxidants. Indeed, the compounds are of interest to technology.[25] Also of note is the ring size effect between the 14-membered **1** and the 12-membered **2**. The smaller ring complexes are consistently easier to oxidize, which may be explained simply on the basis of size; the smaller cavity more greatly stabilizes the smaller oxidized metal ion. Conversely, the larger ligand favors the larger lower valent metal ion; the more difficultly oxidized complexes of **1** contain a metal ion more completely enclosed by the macrobicyclic cavity and more removed from the solvent, as shown in the crystal structure $N_{ax}-M-N_{ax}$ and $N_{eq}-M-N_{eq}$ bond angles (vide supra).

(42) Both iron complexes apparently react with nitromethane; the solutions become increasingly colored with time.

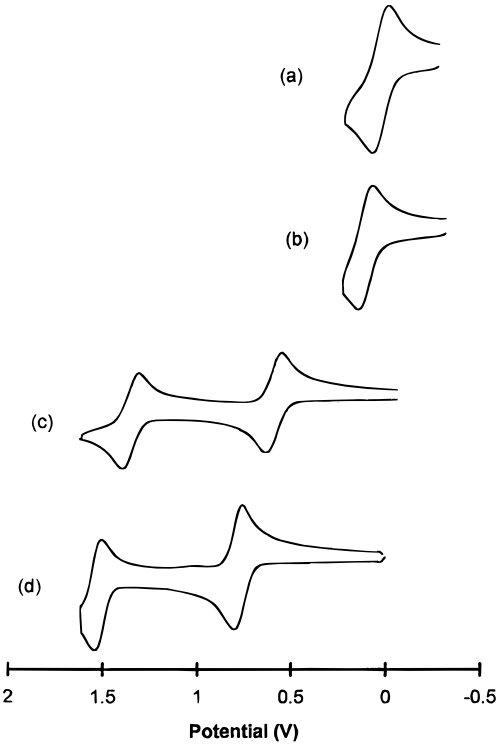


**Figure 11.** Cyclic voltammograms for (a) Fe(**2**)$Cl_2$, (b) Fe(**1**)$Cl_2$, (c) Mn(**2**)$Cl_2$, and (d) Mn(**1**)$Cl_2$.

**Table 5.** Redox Potentials (vs SHE) with Peak Separations

| complex | redox couple | potential (V) | peak separation (mV) |
|---|---|---|---|
| Mn(**1**)$Cl_2$ | $Mn^{II}/Mn^{III}$ | +0.585 | 61 |
| | $Mn^{III}/Mn^{IV}$ | +1.343 | 65 |
| Fe(**1**)$Cl_2$ | $Fe^{II}/Fe^{III}$ | +0.110 | 63 |
| Mn(**2**)$Cl_2$ | $Mn^{II}/Mn^{III}$ | +0.466 | 70 |
| | $Mn^{III}/Mn^{IV}$ | +1.232 | 102 |
| Fe(**2**)$Cl_2$ | $Fe^{II}/Fe^{III}$ | +0.036 | 64 |

**Catalytic Oxidation Studies.** The catalytic efficacy of the $Mn(\mathbf{1})^{2+}$ complex in aqueous solution has been assessed in

**Table 6.** Epoxidation of Carbamazepine[a] in the Presence of Mn(**1**)

| | % conversion of carbamazepine | |
|---|---|---|
| solvent system | $KHSO_5$ (2 h) | $H_2O_2$ (2 h) |
| $H_2O$[b] | 24[c] | 5.1[d] |
| pH 7[b] | 56[c] | 4.4[d] |
| pH 10[b] | 13.1[c] | 17.6[d] |
| $H_2O$/MeOH (1:1) | 6.3[c] | 4.4[d] |
| pH 7/MeOH (1:1) | 11.4[d] | 2.7[d] |
| pH 10/MeOH (1:1) | 5.1[d] | 3.5[d] |

[a] Typical reaction conditions: 0.1 mM Mn(**1**), 4 mM CBZ, 25 mM $KHSO_5$, 50 mM $H_2O_2$, 25 °C. [b] Heterogeneous suspension. [c] Epoxide and diol detected products. [d] Epoxide product only.

epoxidation reactions and hydrogen abstraction reactions. Most earlier studies on catalytic olefin epoxidation have been performed in organic solvents or under biphasic reaction conditions in the presence of phase transfer agents. Epoxidations in aqueous media, which have attracted interest because of their biological significance, are usually confronted by such challenges as limited solubilities of reactants or relatively low product yields. Several publications report[43] metalloporphyrin mediated oxygenation reactions in aqueous/hydroxylic solvents. Carbamazepine (CBZ) is a moderately water soluble substrate suitable for epoxidation studies and was first used by Meunier. CBZ is an antiepileptic drug whose main in vivo metabolites include the epoxide and the corresponding diol. Various terminal oxidants such as $KHSO_5$, $H_2O_2$, *m*-CPBA, and *t*-BuOOH have been employed as oxygen atom surrogates for water-soluble metalloporphyrins. The results of these studies revealed high yields (up tp 100% CBZ conversion) for oxygen transfer reactions in acidic solutions, with decreasing catalytic efficiency at neutral pH up to pH 8.

We have performed oxidation studies on carbamazepine in aqueous solution with several oxidants at various pH values. Under selected experimental conditions, the CBZ solubility in water is limited, resulting in heterogeneous suspensions. Complete homogeneity has been achieved by the addition of methanol to the reaction mixture. The results of our observations on the catalytic oxidation of CBZ with $H_2O_2$ and $KHSO_5$ at various pH values, and in the presence or absence of MeOH, are presented in Table 6. Examination of the data shows that methanol inhibits the oxidation, probably because of the incomplete aquation of Mn(**1**)$Cl_2$ into the corresponding diaqua species. On the time scale of these experiments, no methanol oxidation products have been detected by a well-developed 2,4-dinitrophenylhydrazine test. As expected, the catalytic efficiency with a more potent oxidizing agent, $KHSO_5$, is higher than that with $H_2O_2$. With a variety of terminal oxidants under identical reaction conditions (MeOH/$H_2O$ (1:1 v/v), 0.1 mM Mn(**1**), 1 mM CBZ, 100 mM oxidant, 24 h) CBZ conversion was found to be 76%, 47%, 7.3%, and 2.2% for $KHSO_5$, *m*-CPBA, $H_2O_2$, and *t*-BuOOH, respectively. $H_2O_2$ and *t*-BuOOH produced CBZ-epoxide as the exclusive product, unlike $KHSO_5$ and *m*-CPBA, which also yielded the diol derivative, possibly due to epoxide hydrolysis, and traces of other oxidation products. Unlike the metalloporphyrins, we observed significant oxidation, with epoxide as the sole product, at pH 10, even using $H_2O_2$ as the oxidizing agent. From the data presented here and additional catalyst activation studies,[38] we conclude that Mn $(\mathbf{1})^{2+}$ reacts with terminal oxidants to form Mn $(\mathbf{1})^{4+}$, which then acts as the oxygen transfer agent. Mechanistic investigations of this system and characterization of the active $Mn^{4+}$ intermediate are currently in progress in our laboratories.

A variety of industrial and biochemical processes involve oxidation reactions that proceed via hydrogen atom transfer. As discussed in a recent review by Mayer,[44] catalysts for these processes include organic radicals and metal−oxo complexes, as well as metalloenzymes. The well-known biological processes are assumed to proceed by means of high-valent "M═O" intermediates. The hydrogen atom transfer is accompanied by the reduction of the metal center, and the factors that affect this process include the redox properties of the metal center, the strength of the C−H bond that is being broken, and the strength of the O−H bond being formed. A convenient substrate model for studies of this type of reaction is 1,4-cyclohexadiene (CHD). We have studied the catalytic oxidation of 1,4-cyclohexadiene in the mixed solvent system, MeOH/$H_2O$ (1:1 v/v) with $H_2O_2$ as the terminal oxidant. The analysis of the reaction mixture shows quantitative formation of benzene. Kinetic measurements of CHD disappearance and benzene formation show first-order curves, with the observed rate constants $4.0 \times 10^{-4}$ and $3.8 \times 10^{-4}$ $s^{-1}$, respectively. As was found for the epoxidation reactions, increasing the methanol content from 1:1 to 9:1 (v/v) slows the catalytic process and decreases the yield from 87% to 56%. Under experimental conditions comparable to those used for the CBZ epoxidation (MeOH/$H_2O$ (1:1), 0.1 mM Mn(**1**), 1 mM substrate, and 100 mM oxidant, 2 h) the conversion of CHD was 63.2% and 23.8% with $H_2O_2$ and *t*-BuOOH, respectively. This amounts to approximately 10 times the yield for the oxidation of carbamazepine. From the standpoint of utility, the implicit difference in reactivity toward the two substrates is a demonstration of the selectivity of the oxidation catalysts. For consumer technologies such as laundering, a bleach needs to oxidize stains while leaving dyes unaltered. Understanding the catalytic oxidation mechanisms of the Mn(**1**) complex is the subject of ongoing studies.

## Conclusions

As noted in the Introduction, $Fe^{II}$ and $Mn^{II}$ are enormously important ions in a variety of biological processes. However, their properties have made them difficult to control in oxygenated aqueous systems without the protection of the bulky, hydrophobic proteins provided by nature. The ligands **1** and **2** are designed to do just that: keep $Mn^{2+}$ and $Fe^{2+}$ stable in aqueous solutions and under other harsh conditions to take advantage of their known catalytic reactivity. Here, we have reported the synthesis of $Mn^{2+}$ and $Fe^{2+}$ complexes of the cross-bridged macrobicyclic ligands **1** and **2**, overcoming their proton-sponge nature by reducing the activity of protons in the reaction mixture. Using these simple, but topologically constrained ligands, we have produced complexes which are all high spin yet remarkably stable in various solvents. The extent to which counterions ($Cl^-$) are dissociated increases with the dielectric constant of the solvent resulting in their complete replacement by solvent in water, which produces the two labile cis sites needed for many types of catalysis.[16] The manganese complexes exhibit readily detectable higher oxidation states of +3 and +4, whereas the iron complexes show only the divalent and trivalent states. Such stabilization of multiple oxidation states is again necessary for various catalytic cycles. The coordination spheres of all four divalent metal complexes are comparable, but the smaller ring is more distorted in its pseudo-octahedral complexes

(43) (a) Bernadou, J.; Fabiano, A.-S.; Robert, A.; Meunier, B. *J. Am. Chem. Soc.* **1994**, *116*, 9375. (b) Groves, J. T.; Lee, J.; Marla S. S. *J. Am. Chem. Soc.* **1997**, *119*, 6269. (c) Yang, S. J.; Nam, W. *Inorg. Chem.* **1998**, *37*, 606. (d) Yang, S. J.; Lee, H. J.; Nam, W. *Bull. Korean Chem. Soc.* **1998**, *19*, 276.

(44) Mayer, J. M. *Acc. Chem. Res.* **1998**, *31*, 441.

because these metal ions are a bit larger than would be ideal for occupancy. This is reflected in the electrode potentials and, probably, the kinetic stabilities of the complexes. The derivatives of the larger rings are harder to oxidize, which can be traced to a better size match between the larger ring and the larger di- or trivalent ions and the smaller rings with the smaller tri- or tetravalent ions. Interestingly, the disymmetry of the 14-membered-ring derivative results in a gauche orientation of the *N*-methyl groups while those of the 12-membered-ring derivative adopt the expected eclipsed orientations. The steric consequences of these subtle stereochemical relationships along with the inherent chirality of ligand **1** have not yet been explored. The catalytic efficacies of these new compounds are a matter of immediate interest, having already been applied to aqueous technologies important to consumer products.[25] The catalysts display significant activity while also being selective toward substrates.

**Acknowledgment.** We thank Dr. Martha Morton of the University of Kansas for assistance with the kinetic NMR experiments. The funding of this research by the Procter and Gamble Company is gratefully acknowledged. T.J.H. thanks the Madison and Lila Self-Graduate Research Fellowship of the University of Kansas for financial support. We thank EPSRC and Siemens Analytical Instruments for grants in support of the diffractometer. The Kansas/Warwick collaboration has been supported by NATO.

**Supporting Information Available:** Tables of atomic coordinates and equivalent isotropic displacement parameters, bond distances and angles, anisotropic displacement parameters, and hydrogen coordinates and isotropic displacement parameters for Mn(**1**)$Cl_2$, Mn(**2**)$Cl_2$, Fe(**1**)$Cl_2$, and Fe(**2**)$Cl_2$ (PDF). This material is available free of charge via the Internet at http://pubs.acs.org.

JA990366F